International Journal of Computing and Digital Systems
ISSN (2210-142X)
Int. J. Com. Dig. Sys. 12, No.1 (Sep.-2022)

https://dx.doi.org/10.12785/ijcds/120158

# Comparison Between 2D DCO OFDM and 2D ACO OFDM Systems for Optical Camera Communication

**Noor J. Jihad[1], Sinan M. Abdul Satar[2]**

[1]*Communication Engineering Department, University of Technology-Iraq, Baghdad, Iraq*
[2]*Country Electrical Engineering Department, University of Technology-Iraq, Baghdad, Iraq*

*Received 02 Mar. 2022, Revised 30 Apr. 2022, Accepted 19 Jun. 2022, Published 30 Sep. 2022*

**Abstract:** The influence of changing clipping factors on optical wireless communication (OWC) systems that use orthogonal frequency multiplexing division (OFDM) is discussed in this article. In the present paper, several modulators are available for optical OFDM. A study is undertaken on the two current transmission systems with asymmetrical clipping as well as OFDM with direct current optical DCO OFDM. This investigation examines the comparison between two-dimensional ACO OFDM S2C and DCO OFDM S2C regarding the execution process. This allows us to evaluate all performances without the hardware structure. The selection of the clipped levels has significant effects on the performance of OCC systems. The BER performance (DCO-OFDM S2C OCC) is more efficient concerning the (ACO OFDM S2C OCC) approach for the bit error rate to $10^{-4}$ requirement with the pixel SNR of nearly 18dB. The gain of 3 dB is because, like DCO-OFDM, ACO-OFDM S2C OCC utilizes just lower than the numbers of data carriers. (ACO OFDM S2C OCC system) reduces the PAPRs, at the cost of increasing the bit error rate BER and computations complexities. It shows that the more efficient the BER enhancement. The measurements of the BER for different modes of the OWC system were examined and various clipping factors of 2.9, 2.3, and 3.3. The proposed S2C OCC system was executed by the Lab-view program.
**Keywords:** ACO OFDM S2C, BER, clipping factor, DCO OFDM S2C, OCC, OWC.

## 1. INTRODUCTION

The global Internet of Things (IoT) networks and the abundance of multimedia content for example social media and video content are increasingly calling for optical data [1] . The total mobile traffic would increase to 42 percent of the market demands [2]. The monthly traffic for cell data in 2025 reaches 100 Exabytes (EB). Either bandwidth grows or spectral efficiency improves to satisfy this increasingly increasing demand [3]. However, the increase in spectral efficiency is slow and cannot fulfill the insatiable requirement. Using a new spectrum is an innovative technology because it requires a much broader variety of terahertz (THz) bandwidth [4]. It also observed a major increase in involvement in optical-OFDM from the OWC system. in recent years [5]. Many publications have considerably increased because it was used as an appropriate model of modulation for incoherent transmission detection over long distances and for direct detection [6].

Net data transmission volumes at the experimental level have been rising by a factor of 10 per year in recent years. At present, there has been experimental evidence in one direction, 10.8 TB s1, for transmission of up to 1 Tb s1 on the base of FFT, whereas the DSP is in real-time more than 10 GB s1 [7] for optical OFDM. Such advancements inevitably lead to the development of commercial OFDM-based transmission devices in the future, with theoretically strong spectral efficiency and flexible Architecture for the network [8]. OCC is a network system that employs optical image sensors as IR of OWC communication.

Visible light communication VLC is often considered to be image sensor communication. In comparison to some types of OWC technology, OCC offers several benefits [9]. Initially, there is no adjustment on the Receiver, which includes all possible receiver choices for existing smartphones, video

*E-mail:noor. noor.j.jihad@uotechnology.edu.iq, sinan.m.abdulsatar@uotechnology.edu.iq*

cameras, rear optical, and tracking cameras [10]. Therefore, OCC may facilitate a wide variety of applications. Secondly, millions of pixels of OCC receivers require broad degrees of freedom (DoF), in which data are transmitted to individuals [11] is handled. Thirdly, modern image sensors usually operate on three colors to transmit them in the domain displayed [12]. OCC has attracted considerable interest in areas such as many service applications with a high capacity [13]. Thus, the OCC constraints are restricted but are not restricted to the small recipient sampling size, off-focus effect, inaccurate frame rate, and randomization [15]. To overcome these limitations, the OCC research community has built many approaches [16]. The transceiver system (bidirectional communication system) has been connected back-to-back communication system. The study will be focused on the implementation of the OCC for the two-dimensional two modes of optical OFDM for the literature on OFDM for the implementation of the OCC. A BER measurement will be presented in the second section for two forms of optical OFDM.

## 2. 2D-OFDM S2C OCC SYSTEMS

OWCs are a promising standard for establishing lower-speed information transfers. Contact with infrared and visible light was capable of providing many hundred Mbps [17]. OWC benefits from license-free operation over a far greater variety of devices as well as provides a suitable method that does not overlap with RF technology. In OWC, (IM / DD) ensures data transport [18].

A positive, real frequency increases the LED intensity of the LED in the transmitter and is detected by photo-detectors in the receivers. [30]. The inherent robustness of the multi-path dispersion of the Wireless optical Channels in the MCM modulation of the M-QAM OOFDM is expected to deliver very higher data transmission rates [19]. In the paper, two possible system achievements of OFDM screen-camera systems can be found: DCO OFDM S2C/OCC and ACO-OFDM S2C/OCC systems. When Hermitians symmetries are applied to OFDM subcarriers, a properly assessed signal is obtained[20].

The 2D-DTFT is common and defined as a usual conversion:

$$F(u,v)=\sum_{n=-\infty}^{\infty}\sum_{m=-\infty}^{\infty}f[m,n]e^{-j2\pi(um+vn)} \quad (1)$$

$$F(k,l)=\frac{1}{MN}\sum_{m=0}^{M-1}\sum_{n=0}^{N-1}f[m,n]e^{-j2\pi\left(\frac{K}{M}m+\frac{l}{N}n\right)} \quad (2)$$

Given the theoretical description of Discrete-Time Fourier Transform DTFT and Discrete Fourier Transform, the 2D-DFT might be described as a sampled variation of 2D-DTFT. Furthermore, for the predicted bi-dimensional structure of this mean S2C system, it is important to leave the 2D-DFT for the images as follows.: [29]

$$F(k,l)=\frac{1}{\sqrt{MN}}\sum_{n=0}^{M-1}\sum_{m=0}^{M-1}f[m,n]e^{-j2\pi\left(\frac{K}{M}m+\frac{l}{N}n\right)} \quad (3)$$

This is followed by the 2D IDFT as observes

$$F(m,n)=\frac{1}{\sqrt{MN}}\sum_{K=0}^{M-1}\sum_{K=0}^{M-1}F[k,l]e^{j2\pi\left(\frac{K}{M}m+\frac{l}{N}n\right)} \quad (4)$$

For m ranges from 0 to M-1 and n ranges from 0 to N-1. A shift 2D-DFT transform is the shift variation of a conventional 2D-DFT, which will almost certainly not be noticed. The symmetric feature of the discrete Fourier transforms in two dimensions is the same as that of the IDFT in one dimension[8].

$$(m,n)=\frac{1}{\sqrt{MN}}\sum_{k=0}^{M-1}\sum_{k=0}^{N-1}F[m,n]e^{-j2\pi\left(\frac{K}{M}m1+\frac{l}{N}n1\right)} \quad (5)$$

$$F(m,n)=\frac{1}{\sqrt{MN}}\sum_{k=0}^{M-1}\sum_{k=0}^{N-1}F[m,n]e^{-j2\pi\left(\frac{K}{M}m2+\frac{l}{N}n2\right)} \quad (6)$$

Between the 2D carriers, the orthogonally represented as follows:

$$f\,[m1,n1]\perp f[m2,n2],(m1\neq m2)\vee(n1\neq n2)$$

The clipping factor selection is crucial to the results, as it has a direct impact on the implementation outcomes. The clipped levels are experimentally selected [8].

### *A. DCO-OFDM*

The specific functional blocks are defined as follows in the DCO-OFDM framework, in particular for the ACO-OFDM. Bits are mapped into a complicated collection of integers via QAM mapping. Hermitian mappings can form two matrices of imaginary numbers from a sequence of mathematics in a manner that 2D-IDFT accuracy is assured.


Figure.1 DCO-OFDM Schematic of the transmitter part [8]

DC-bias is used to increase the IDFT's output to a minimum amplitude larger than zero. Unlike ACO-OFDM, which drives all negative values to zero, this approach of adding DC-bias in DCO-OFDM is used to transmit all positive and negative outputs from the IDFT. Clipping and ranging shall cope with PAPR fluctuation and shall adjust the clipping thresholds prepared to be conveyed [24]. Fig.1 displays the DCO-OFDM transmitter part assuming that the sub-carriers are assigned in a particular OFDM frame. The sequential bits frames at the transmitter are first changed to the parallel order. In addition, it is plotted to the N/2 − 1 complex value symbol. For unique constellation modulation X, such as modulation of the quadrature amplitude (QAM)[8]. The modulated X = [X0 X1 ……XN−1] OFDM node, where the subscript number indicates the subcarrier index associated with it, as shown in the following equations:

X0 = 0 and X1 to XN/2−1 are symbolized with N/2 − 1 details, while XN/2.In XN−1 the Hermitian symmetry satisfies as:[25]

$$X_K = X^*_{N-K}, k = \frac{N}{2}, \dots \dots N-1, \quad (7)$$

Where the superscript "*" symbolizes conjugate action. It is selected that $X_0 = X_{N/2} = 0$ is intended to avoid the complex harmonics DC components.

The OFDM symbol vector X is provided for the fast inverse Fourier transform (IFFT):[25]

$$x_n = \frac{1}{\sqrt{N}} \sum_{k=0}^{N-1} X_k \exp\left(j\frac{2\pi kn}{N}\right), n = 0,1, \dots . N-1, \quad (8)$$

Where $x_n$ illustrate the $nth$ DFT samples which were displayed the Hermitian symmetry, the operations of the IFFT could be stated as [8]

Thus, opposite to ACO-OFDM, DCO-OFDM assigns data to all 2D Hermitian matrix subcarriers. Cyclic prefix covering the dimensional OFDM symbols is also applied to shield the sign from interaction with the symbol. The cyclic prefix insertion is similar to the ACO OFDM S2C program. Figure 1 display a practical block diagram for implementing spatial DCO-OFDM [22].

$$x_n = \frac{1}{\sqrt{N}} \sum_{k=1}^{N/2-1} \left(X_k \exp\left(j\frac{2\pi kn}{N}\right) + X_{N-K} exp\left(j\frac{2\pi k(N-K)n}{N}\right)\right) \quad (9)$$

$$= \frac{1}{\sqrt{N}} \sum_{k=1}^{\frac{N}{2}-1} \left(X_k \exp\left(j\frac{2\pi kn}{N}\right) + X_k^* exp\left(-j\frac{2\pi k\, n}{N}\right)\right) \quad (10)$$

$$= \frac{2}{\sqrt{N}} \sum_{k=1}^{N/2-1} Re\left(X_k \exp\left(j\frac{2\pi kn}{N}\right)\right) n = 0,1, \dots . N-1 \quad (10)$$

Where Re (Z) belongs to the actual element of Z. Finally, it should be emphasized that N/2-1 is the cumulative subcarrier used and the remaining subcarriers are used to determine Hermitian symmetry. Following IFFT, the cyclic length LCP prefix is changed to the front. CP produces guard intervals by the lack of the orthogonality of subcarriers.CP produces guard intervals by the lack of the orthogonality of subcarriers [21]. The effective multi carriers and simple design are DCO-OFDM for VLC transmission. However, it has an innate lack of proper power efficiency. This is because moving a negative peak above zero needs a high degree of DC bias. This generates a substantial loss of power performance, reducing the acceptable reliability of the DCO-OFDM systems.

### *B. ACO-OFDM*

A functional block diagram to include spatial ACO-OFDM is shown in Fig.2 for the spatial ACO-OFDM system, notably for the ACO-OFDM screen. QAM mapping is designed to show the bit series to a real number sequence (one-dimensional order), Hermitian mappings architecture of a bi-dimensional matrix of Complex numbers from a sequence of Complex numbers to verify the performance of the 2D-IDFT is totally real.


Figure.1 DCO-OFDM Schematic of the transmitter part [8]

The addition of the CP is to maintain the OFDM space in the space domain and prevent symbols from interacting with other symbols, this phenomenon is called intersymbol interference ISI. 2D-IDFT negative symbols are set to zero. [5]. ACO- OFDM block diagram is

identical to its equivalent DCO-OFDM. The distribution of data symbols is a huge difference. Information symbol is simply set on the odd subcarrier of the first N/2 subcarriers in the ACO-OFDM scheme and can thus I[5]. The ACO-OFDM diagram is similar to the DCO-OFDM block diagram. There is a substantial difference in the set of data symbols. In the ACO-OFDM system, the information symbol is simply placed on the odd sub-carrier of the first N/2 subcarriers, and hence the ACO-OFDM block of N subcarriers only allows N/4 information symbols. In terms of real-value amplitude, the Hermitian symmetry restriction of Equ.7 is likewise enforced on the (N/2)th to (N1)th subcarriers. Following the IFFT process, the discrete time-domain sample necessitates the use of transmitters[25].

$$x_n = \frac{1}{\sqrt{N}}\sum_{k=0}^{N-1}\left(X_k \exp\left(j\frac{2\pi kn}{N}\right)\right) \quad (11)$$

$$x_n = \frac{1}{\sqrt{N}}\sum_{k=0}^{N-1}\left(X_{2m+1}\exp\left(j\frac{2\pi(2m+1)n}{N}\right)\right) \quad (12)$$

$$= -\frac{1}{\sqrt{N}}\sum_{k=0}^{N/2-1}\left(X_{2m+1}\exp\left(j\frac{2\pi(2m+1)(n+\frac{N}{2})}{N}\right)\right)$$

$$= -x_n + \frac{N}{2}, n = 0,1,\ldots.N-1, \quad (13)$$

The asymmetry in Equ.14 confirms the idea that the amplitudes of the first half samples are similar, however with opposite symbols, to those of the second half samples. The negative-valued $x_n < 0$ By observing the asymmetry sample, it is possible to recover $x_n + N/2$ or $x_n - N/2$. Therefore, without inserting any DC bias, the ACO-OFDM signal $x_{ACO}(t)$ is completely clipped at zero and then converted into optical signals. Supposing that the clipped sample is $x_n^c$, as seen in the following equations:

$$x_n^c = \begin{Bmatrix} x_n & if\ x_n > 0 \\ 0 & if\ x_n < 0 \end{Bmatrix} \quad (14)$$

The distorted Symbols of Data $x_{2m+1}^c$ on the odd subcarriers $m = 0, 1, \ldots, N/2 - 1$ will be stated as:

$$x_{2m+1}^c = \frac{1}{\sqrt{N}}\sum_{n=0}^{N-1}\left(x_n^c\, exp\left(-j\frac{2\pi(2m+1)n}{N}\right)\right)$$

$$= \frac{1}{\sqrt{N}}\sum_{n=0}^{N/2-1}\left(x_n^c - x_n^c + N/2)exp\left(-j\frac{2\pi(2m+1)n}{N}\right)\right)$$

$$= \frac{1}{2\sqrt{N}}\sum_{n=0}^{N/2-1}\left(x_n - x_n + N/2)exp\left(-j\frac{2\pi(2m+1)n}{N}\right)\right)$$

$$= \frac{1}{2\sqrt{N}}\sum_{n=0}^{\frac{N}{2}-1}\left(x_n\, exp\left(-j\frac{2\pi(2m+1)n}{N}\right)\right)$$

$$+ \frac{1}{2\sqrt{N}}\sum_{n=0}^{N/2-1}\left((x_n + N/2)exp\left(-j\frac{2\pi(2m+1)(n+\frac{N}{2})}{N}\right)\right)$$

$$= \frac{1}{2}x_{2m+1} \quad (15)$$

## 3. HERMITIAN MAPPING

all symbols are first ordered into a Hermitian 2D matrix, rather than immediately passing the mapping symbols to the Inverse fast Fourier. In 2D IFFT, the matrix is then fed into the product's defining qualities. The Hermitian structure guarantees that the IFFT's output is true. To understand the mapping procedure, keep in mind that complex numbers are a = (x+ iy), and the complex number combination $\bar{a}$ = (x – iy).

### *A. ACO-OFDM Hermitian mapping*

Both even-index columns in ACO-OFDM are considered to be zero to ensure that the 2D-IFFT block findings are correct. (even subcarrier). Fig.3 shows the symbol size of the ACO-OFDM. The mapped symbols generated by QAM are in the odd columns (known as odd subcarrier). The Hermitian symmetry is illustrated as follows:

$$X_{i,j} = \overline{X_{M-i,N+1-J}} \quad (16)$$

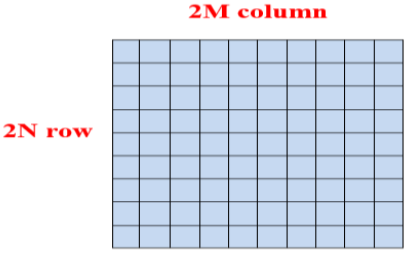


Figure 3.ACO OFDM symbol size

This means the matrices are conjugated symmetrical via the center point.

*B. DCO-OFDM S2C OCC Hermitians mappings*

Assume that the Hermitian matrix has a size of (2k+1) x (2k+1) and that the (2k2+2k) =2k(k+1) complex numbers. The 2D-IFFT must create (2k+1)(2k+1) real values to be shown in an 8-bit matrix [8].

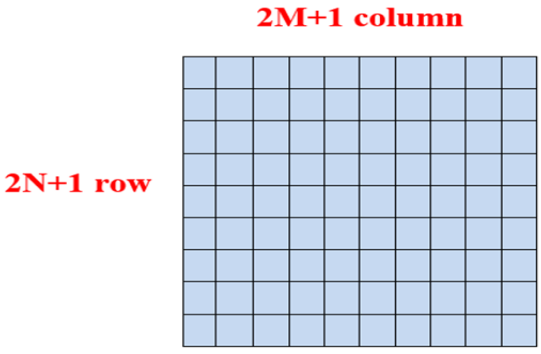


Figure.4 DCO OFDM symbol size[8]

The Hermitian matrix has the same size as the real values following the 2D-IFFT operation. Figure.4 MIMO-OFDM symbol generation; based on the desired resolutions, the size of the 2D Hermitian mappings ((2k+1) x (2k+1)) could be measured.

## 4. SYSTEM SETUP

The 2D OFDM OCC system functional block diagram is observed in Figure 5. This part refers to the optical OFDM system output test using lab view 2019 software in an OCC system. This research has introduced a bidirectional optical OFDM S2C OCC. The text displayed shows the objectives of the UOT/ Baghdad/Iraq as presented in Figure 6.

Fig.5 shows that the proposed configuration consists of two OFDM optical modes, ACO OFDM S2C OCC and DCO-OFDM S2C OCC, to compare the results of BER. Additionally, the efficiency reduction schemes of the PAPR should be assessed in two subsequent parts. Aspects that change the clipping factors that encode and encode the result for BER. Fig.6 shows the receiver's decoded text and the inside TX without the need for a cyclic prefix CP and noise, The CP cyclic prefix is intended to reduce interference between OFDM signals [26].

In addition, Fig.7 shows the transmitter code of the encoded data. The inner section of the Tx. Also has a manageable clock rate for varying the TX processing rate.

Additionally, PAPR performance enhancement systems can be tested in two respects that change the ACO-OFDM S2C OCC and DCO-OFDM S2C OCC clipped levels as well as the coding and encoding of BER performance. The connection between ACO-OFDM and DCO-OFDM is further discussed in this part using the BER compared with the SNR in data transfer despite the data transmission, a single bit of errors can occur within received bits.

## 5. SIMULATIONS DESIGNS

Both forms of OFDM S2C OCC, ACO-OFDM, and DC OFDM are presented in the next sections. Fig.8 BER presentation of (a)ACO OFDM S2C OCC, and (b) DCO OFDM S2C OCC at 2.3 clipping factor shows that depending on the pixel SNR, the clipping factor was modified for optimal BER. The results of error measurements in 2 layers, the first layer with no error correction, and the second layer with convolutional coding forward error correction CC FEC. This shows also that the BER for the system output at the CC is better than the BER. The following section also included just a few BER performances:

The clipping technique is an effective system of average reduction in PAPR power to peak, restricting the maximum signal transmissions to a predetermined value. Figure.8 BER performance of (a)ACO OFDM,(b) DCO OFDM at 2.3 .

However, the following disadvantages are caused by clipping distortion, which results in performance degradation of BER. Fig.10 shows that after increasing the clipping factor to 3.3, the BER performance of ACO OFDM will improve, and the SNR will increase to 15 dB, with the BER $10^{-4}$, which is much better than the BER performance compared to [8].

As can be observed, the BER at 2.3 clipping factor was $10^{-4}$, but the BER at the expense of the SNR is around 17 dB. Figure 10 shows the BER performance of (a) ACO OFDM and (b) DCO OFDM at a 3.3 clipping factor. This is because with a given amount of samples, there is an error-free threshold, and there is an SNR threshold where you have the error[28]. The selection of a clipping factor is critical to the final output and has a direct influence on system performance. When comparing real BER curves, it is demonstrated that the performance of ACO OFDM is more reliable than that of DCO-OFDM. It is observable:

- Reducing the PAPR for the ACO OFDM system as the consequence of the BER bit error enables higher design, coding and decoding, and so on.
- The BER measurements of DCO-OFDM are more efficient related to the ACO OFDM system concerning BER $10^{-4}$, SNR nearly 18dB requirement. In addition, the clipped levels selection is important and has a straight influence on systems efficiency.
- All the simulation shows, that the smaller the clipped rate enhanced the PAR reduction performance, and the worse the BER performance.

- In comparison to DCO-OFDM, ACO-OFDM utilizes only half the number of two-dimensional sub-carriers for data.

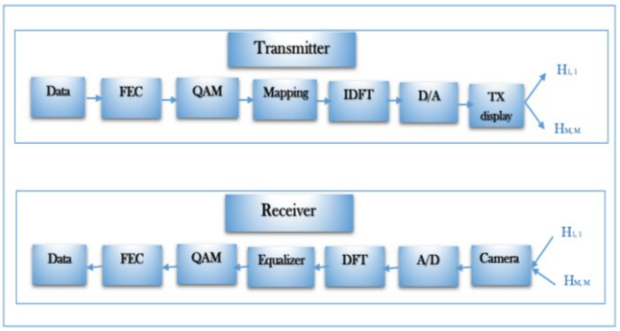


Figure 5. proposed OFDM OCC S2C system

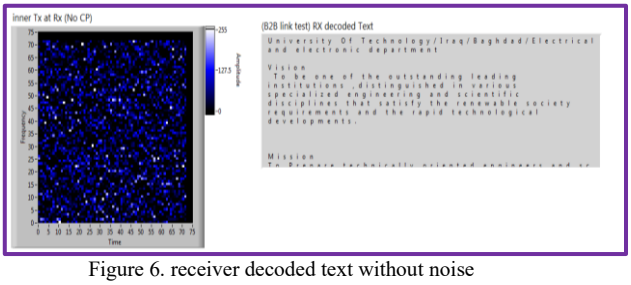


Figure 6. receiver decoded text without noise

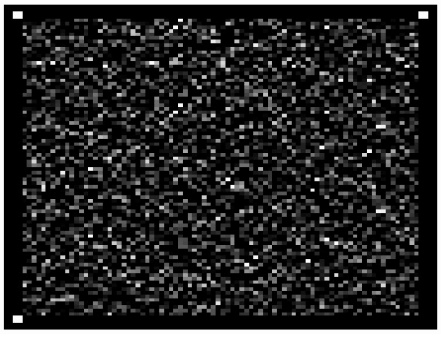

Figure 7. Transmitter code

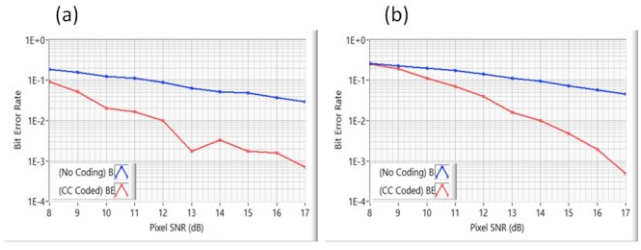


Figure 8.SNR versus BER performance of (a)ACO OFDM S2C,(b) DCO OFDM S2C at 2.3 clipping factor

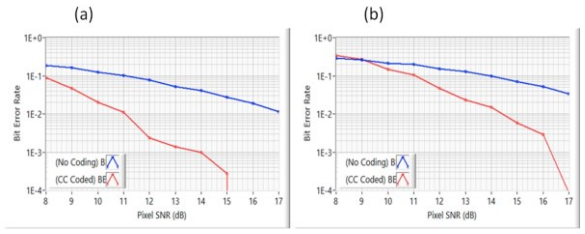


Figure 9. SNR versus BER measurements of (a)ACO OFDM S2C OCC,(b) DCO OFDM S2C OCC at 2.9 clipping factor

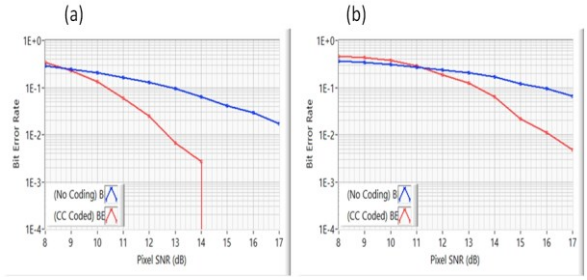


Figure 10. SNR versus BER measurements of (a)ACO OFDM S2C OCC,(b) DCO OFDM S2C OCC at 3.3 clipping factor.

## 6. CONCLUSION

Optical OFDM S2C/OCC systems were implemented for the system in this research. Additionally, the PAPR decline and the bit error rate of different modes of optical OFDM are also discussed to test the influence on OCC system performance. This is done by changing the clipping factors. It suggested a technique to reduce the signal-to-noise ratio by determining the optimal clipping factors. Implementation Results obtained show that a large increase in the SNR ratio for ACO OFDM S2C OCC and DCO OFDM S2C OCC systems is achieved by the selection process with the optimum clipping ratio. The conclusion is that a lower clipping (more robust communication performance) factor is better for low SNR. Compared to the practical BER curves, DCO OFDM's performance is more reliable than the ACO-OFDM S2C system.

The clipped level choice is important and has a straight effect on system performance. The performance of BER versus received SNR deteriorates with increasingly nonlinear distortions as the clipping ratio decreases. The main issue addressed in this paper is to ensure that the signals are appropriately generated and to determine what elements may impact the system's performance if the transceiver system back-to-back communication system has been connected. It is also determined that the higher the noise of the clipping process will reduce the PAPR by the clipping ratios decrement to SNR at the expense of the decrease in BER to $10^{-4}$. Additionally, BER performance for both optical OFDM modes will be enhanced with the coding of convolutional forward error correction.

## ACKNOWLEDGMENT

I would like to express my thanks to prof. Sinan M. Abdul Satar has assisted me at every stage of my study. I'd also want to offer my gratitude and appreciation to the optical press team of all those who supported me at every stage of my study work, as well as my colleagues, for their continuous love and care. Thank Allah, the Almighty, for assisting me in overcoming all of the challenges that have come my way.

## REFERENCES

[1] M. Young, The Technical Writer's Handbook. Mill Valley, CA: University Science, 1989. E. Vanin, "Performance evaluation of intensity-modulated optical OFDM system with digital baseband distortion", Optics Express, vol. 19, no. 5, p. 4280, 2011. Available: 10.1364/oe.19.004280.

[2] N.J. Jihad,S.M. Abdul satar," Performance evaluation of error correction for screen-camera communication systems",Opt Quant Electron,vol.54,no.100,2022.Available: https://doi.org/10.1007/s11082-021-03452-3[Accessed 20 March 2022].

[3] S. Dissanayake and J. Armstrong, "Comparison of ACO-OFDM, DCO-OFDM and ADO-OFDM in IM/DD Systems", Journal of Lightwave Technology, vol. 31, no. 7, pp. 1063-1072, 2013. Available: 10.1109/jlt.2013.2241731

[4] M. Mondal, "Comparison of DCO-OFDM, ADO-OFDM, HDC-OFDM and HNC-OFDM for Optical Wireless Communications", Journal of Optical Communications, vol. 0, no. 0, 2018. Available: 10.1515/joc-2018-0073 [Accessed 20 May 2020].

[5] 贾. Jia Kejun, 靳. Jin Bin, 郝. Hao Li and 张. Zhang Shouqin, "Performance Analysis of DCO-OFDM and ACO-OFDM Systems in Indoor Visible Light Communications", Chinese Journal of Lasers, vol. 44, no. 8, p. 0806003, 2017. Available: 10.3788/cjl201744.0806003 [Accessed 20 May 2020].

[6] S. Manoj, "A Novel 2D ASCO-OFDM Scheme In Wireless Communication", International journal of Emerging Trends in Science and Technology, 2016. Available: 10.18535/ijetst/v3i03.10 [Accessed 20 May 2020].

[7] A. Ali Qasim , M. F. L Abdullah, H. Noman Mohammedali, R. Bin Talib. M. N. Nemah, A. T. Hammoodi," Low complexity DCO-FBMC visible light communication system", International Journal of Electrical and Computer Engineering (IJECE), Vol. 10, No. 1, February 2020, pp. 928~934 ISSN: 2088-8708, DOI: 10.11591/ijece. v10i1.pp928-934.

[8] T. Nguyen, M. Thieu and Y. Jang, "2D-OFDM for Optical Camera Communication: Principle and Implementation", IEEE Access, vol. 7, pp. 29405-29424, 2019. Available: 10.1109/access.2019.2899739 [Accessed 20 May 2020].

[9] Z. Gebeyehu, "Impact of clipping noise on the sum rate of NOMA with PD-DCO-OFDM and conventional DCO-OFDM", Heliyon, vol. 6, no. 2, p. e03363, 2020. Available: 10.1016/j.heliyon.2020.e03363 [Accessed 20 May 2020].

[10] J. Koti and B. Mishra, "BER Performance Comparison of DCO-OFDM and Convolutional Coded DCO-OFDM in IM/DD Systems", International Journal of Electronics, Communications, and Measurement Engineering, vol. 8, no. 2, pp. 26-39, 2019. Available: 10.4018/ijecme.2019070102 [Accessed 20 May 2020].

[11] J. Lain, Z. Yang and T. Xu, "Experimental DCO-OFDM Optical Camera Communication Systems With a Commercial Smartphone Camera", IEEE Photonics Journal, vol. 11, no. 6, pp. 1-13, 2019. Available: 10.1109/jphot.2019.2948071.

[12] Y. Zang and J. Zhang, "Optimal Scheme of DCO-OFDM for Optical Frequency-selectivity", Procedia Computer Science, vol. 131, pp. 1074-1080, 2018. Available: 10.1016/j.procs.2018.04.261 [Accessed 20 May 2020].

[13] R. Hema, S. Sudha and K. Aarthi, "Performance studies of MIMO based DCO-OFDM in underwater wireless optical communication systems", Journal of Marine Science and Technology, 2020. Available: 10.1007/s00773-020-00724-7.

[14] Jihad, N.J., Abdul satar, S.M. Two-dimensions asymmetrically clipped optical orthogonal frequency division multiplexing for screen to a camera communications system. Opt Quant Electron 53, 376 (2021).

[15] Anas A. Hussien, Adnan H. Ali, "Comprehensive investigation of coherent optical OFDM-RoF employing 16QAM external modulation for long-haul optical communication system," *International Journal Electrical and Computer Engineering (IJECE),* vol. 10, no. 3, pp. 2607-2616, 2020.

[16] J. Ratnam and S. Mali, "Impact of Rayleigh-Distributed PAPR on the Performance of a Pre-Clipped DCO-OFDM System", Journal of Optical Communications, vol. 0, no. 0, 2019. Available: 10.1515/joc-2019-0097.

[17] F. Tithi and S. Majumder, "Performance analysis of a DCO-CO-OFDM optical transmission system with distributed Raman amplifier using coherent heterodyne receiver", Optik, vol. 210, p. 164481, 2020. Available: 10.1016/j.ijleo.2020.164481 [Accessed 20 May 2020].

[18] J. Padhy and B. Patnaik, "CO-OFDM and DP-QPSK Based DWDM Optical Wireless Communication System", Journal of Optical Communications, vol. 0, no. 0, 2018. Available: 10.1515/joc-2018-0072 [Accessed 20 May 2020].

[19] Jihad, Noor J., and Sinan M. Abdul Satar. "BER performance study for optical OFDM of optical camera communication." International Journal of Electrical & Computer Engineering (2088-8708) 11.5 (2021).

[20] Luo, "A Rotated Constellation Aided OFDM System for Wireless Communication", International Journal of Performability Engineering, 2018. Available: 10.23940/ijpe.18.12.p32.32283236 [Accessed 25 May 2020].

[21] R. Miglani and J. Malhotra, "Investigation on R–S Coded Coherent OFDM Free Space Optical (CO-OFDM-FSO) Communication Link Over Gamma–Gamma Channel", Wireless Personal Communications, vol. 109, no. 1, pp. 415-435, 2019. Available: 10.1007/s11277-019-06571-z [Accessed 25 May 2020]

[22] J. Lee, J. Kim and W. Kim, "Comparison and Performance analysis of Wavelet OFDM system and FD-OFDM", Journal of the Institute of Electronics and Information Engineers, vol. 50, no. 7, pp. 34-42, 2013. Available: 10.5573/ieek.2013.50.7.034 [Accessed 20 May 2020].

[23] R. Daniels and R. Heath, "Modeling ordered subcarrier SNR in MIMO-OFDM wireless links", Physical Communication, vol. 4, no. 4, pp. 275-285, 2011. Available: 10.1016/j.phycom.2011.10.001 [Accessed 25 May 2020].

[24] Q. Luo, "A Rotated Constellation Aided OFDM System for Wireless Communication", International Journal of Performability Engineering, 2018. Available: 10.23940/ijpe.18.12.p32.32283236 [Accessed 25 May 2020].

[25] M. H. Ali, A. H. Ali, S. M. Abdulsatar, M. A. Saleh, A. K. Abass, and T. F. Al-Mashhadani, "Pump power optimization for hybrid fiber amplifier utilizing second-order stimulated Raman scattering," Opt Quant Electron, vol. 52, no. 6, Jun. 2020.

[26] M. H. Ali, A. K. Abass, and S. A. Abd Al-Hussein, "32 Channel × 40 Gb/s WDM optical communication system utilizing different configurations of hybrid fiber amplifier," Opt Quant Electron, vol. 51, no. 6, p. 188, Jun. 2019.

[27] Jihad, Noor J., and Sinan M. Abdul Satar. "Performance study of ACO-OFDM and DCO OFDM in optical camera communication

system." In 2020 2nd Al-Noor International Conference for Science and Technology (NICST), pp. 63-67. IEEE, 2020.

[28] Yaseen, Mohammed Ali, A. K. Abass, and Sinan M. Abdulsatar. "Improving of Wavelength Division Multiplexing Based on Free Space Optical Communication via Power Comparative System." *Wireless Personal Communications* (2021): 1-11.

[29] Al-Hashime, Liqaa A., Ghaida A. Al-Suhail, and Sinan M. Abdul Satar. "Modulation Mapping Influence in Coherent Optical OFDM System for Long Haul Transmission." In International Conference on New Trends in Information and Communications Technology Applications, pp. 193-209. Springer, Cham, 2018.

[30] Jihad, Noor J., and Sinan M. Abdul Satar. "Optical Camera Communication Performance Evaluation." IRAQI JOURNAL OF COMPUTERS, COMMUNICATION, CONTROL & SYSTEMS ENGINEERING 20, no. 3 (2020).

**Noor J. Jihad** was born in Baghdad, Iraq. I graduated from the University of Technology with a Bachelor's degree (First Rank) in electrical and electronics engineering in 2009. I received a Master's degree with distinction in communications engineering from Brunel University London in 2012. My scientific degree is a Lecturer since 2014. Currently, I am one of the staff of the communication engineering department at the University of Technology, Baghdad, Iraq, and a Ph.D. student at UOT Baghdad, Iraq. My Research Interests: optical camera communication systems, optical wireless communication systems, optical fiber Communications engineering Systems, modern Communications Systems .wireless, and Microwave engineering.

**Sinan M. Elias** was born in Baghdad, Iraq in 1970. He received his B. Sc and M.Sc degrees in 1993 and 1998 respectively from MEC, Iraq. From 2003-2006, he joined a Ph.D. study at the Faculty of Electrical and Electronics Engineering, University of Technology, Iraq. Since 2012, he has been an Assistant Professor of Electronics and Communications Eng. At the UOT, Iraq. From 2018 until now, Dr. Elias headed the Electronic branch at the electrical department, University of technology. He started scientific publishing in 2000, he has more than 37 publications in national and international conferences and journals. Dr. Sinan is IEA and ILS member.